UNIVERSITY OF TURKU

# Real-Time Simulation and Control of an EV Traction Motor in a HIL-environment

Department of Mechanical and Materials Engineering

Bachelor's thesis

Author:
Jenna-Maria Valkeinen

13.5.2026

Turku

Bachelor's thesis

**Subject**: Automation Engineering
**Author**: Jenna-Maria Valkeinen
**Title:** Real-Time Simulation and Control of an EV Traction Motor in a HIL-environment
**Supervisor**: Prof D.G. Dorrell
**Number of pages**: 30 pages
**Date**: 13.5.2026

The purpose of this thesis is to develop and analyse a real-time simulation model for an electric vehicle (EV) powertrain in the Typhoon HIL environment. The study focused on a modern EV Hyundai Ioniq 5 and its interior permanent magnet synchronous motor (IPMSM). The literature review consists of key components of an EV, the fundamentals and working principle of the PMSM and information of high-voltage system and driving cycles.

The experimental section utilizes real-time Hardware-in-the-loop (HIL) technology. An electric drivetrain model, including the battery, inverter, IPMSM, and vehicle dynamics is constructed. The control logic is implemented using the FOC algorithm, and the model's functionality is validated through WLTP-cycle. The results are analysed by comparing the control commands to the actual motor behaviour. Discrepancies identified during the simulation, such as synchronization challenges in the electrical angle ($\theta$), are analysed and development recommendations are considered to enhance the accuracy of motor control in real-time simulation.

**Key words**: PMSM, Typhoon HIL, Real-time simulation, Electric Vehicle, Driving Cycle

Kandidaatintutkielma

**Oppiaine**: Automaatiotekniikka
**Tekijä**: Jenna-Maria Valkeinen
**Otsikko:** Real-Time Simulation and Control of an EV Traction Motor in a HIL-environment
**Ohjaaja**: Professori D.G. Dorrell
**Sivumäärä**: 30 sivua
**Päivämäärä**: 13.5.2026

Tämän kandidaatintutkielman tarkoituksena on kehittää ja analysoida sähköauton voimalinjan reaaliaikaista simulaatiomallia Typhoon HIL-ympäristössä. Tutkimus keskittyy nykyaikaiseen Hyindai Ioniq 5 -sähköautoon ja sen hyödyntämään kestomagneettimoottoriin (IPMSM, engl. Interior Permanent Magnet Synchronous Motor). Kirjallisuuskatsauksessa tarkastellaan sähköauton keskeisiä komponentteja, kestomagneettimoottorin toimintaperiaatteita sekä korkeajännitejärjestelmiä ja ajosyklejä.

Kokeellisessa osiossa hyödynnetään reaaliaikaista Hardware-in-the-loop (HIL) -teknologiaa. Työssä rakennetaan sähköisen voimalinjan malli, joka sisältää akun, taajuusmuuttujan, kestomagneettimoottorin sekä ajoneuvodynamiikan. Ohjauslogiikka toteutetaan hyödyntäen kenttäorientoitua ohjausta (FOC, engl. field-oriented control) ja mallin toiminnallisuus varmennetaan WLTP-ajosyklillä. Tuloksia analysoidaan vertaamalla ohjauskomentoja moottorin todelliseen käyttäytymiseen. Simulaation aikana havaitut poikkeamat, kuten sähköisen kulman $\theta$ synkronointiin liittyvät haasteet, analysoidaan sekä lopuksi tarkastellaan kehitysehdotuksia moottorin ohjauksen tarkkuuden parantamiseksi reaaliaikaisessa simulaatiossa.

**Avainsanat**: kestomagneettimoottori, Typhoon HIL, reaaliaikainen simulointi, sähköauto, ajosykli

List of used symbols:

| | | |
|---|---|---|
| $\boldsymbol{I_a, I_b, I_c}$ | Phase currents | A |
| $\boldsymbol{I_{ref}}$ | General reference current | A |
| $\boldsymbol{i_d, i_q}$ | d-axis and q-axis current | A |
| $\boldsymbol{i_{q,ref}}$ | q-axis reference current | A |
| $\boldsymbol{v_{ref}}$ | Reference vehicle velocity | m/s |
| $\boldsymbol{\omega_{ref}}$ | Motor reference angular speed | rad/s |
| $\boldsymbol{I}$ | Current | I |
| $\boldsymbol{L_d, L_q}$ | d-axis and q-axis inductances | H |
| $\boldsymbol{L\_q}$ | q-axis Inductance | H |
| $\boldsymbol{P}$ | Power | W |
| $\boldsymbol{Q}$ | Electric charge | Ah |
| $\boldsymbol{R_s}$ | Stator resistance | Ω |
| $\boldsymbol{T}$ | Torque | Nm |
| $\boldsymbol{V}$ | Voltage | V |
| $\boldsymbol{\theta}$ | Electrical angle | rad |

List of used abbreviations:

| | |
|---|---|
| **AC** | Alternating Current |
| **BLDC** | Brushless Direct Current Motor |
| **BMS** | Battery Management System |
| **CLTC** | China Light-Duty Vehicle Test Cycle |
| **CPU** | Central Processing Unit |
| **DC** | Direct Current |
| **EMF** | Electromagnetic Field |
| **EPA** | Environmental Protection Agency |

| | |
|---|---|
| **EV** | Electric Vehicle |
| **FOC** | Field-oriented Control |
| **FPGA** | Field-Programmable Gate Array |
| **HIL** | Hardware-in-the-loop |
| **ICE** | Internal Combustion Engine |
| **IM** | Induction Motor |
| **IPMSM** | Interior Permanent Magnet Synchronous Motor |
| **MF** | Magnetic Field |
| **MTPA** | Maximum Torque per Ampere |
| **MTPV** | Maximum Torque per Volt |
| **NaN** | Not-a-Number |
| **NEDC** | New European Driving Cycle |
| **PC** | Personal Computer |
| **PI** | Proportional Integral |
| **PMSM** | Permanent Magnet Synchronous Motor |
| **PWM** | Pulse Width Modulation |
| **RPM** | Revolutions per Minute |
| **SCADA** | Supervisory Control and Data Acquisition |
| **SPMSM** | Surface Permanent Magnet Synchronous Motor |
| **SRM** | Switched Reluctance Motor |
| **SVPWM** | Space Vector Pulse Width Modulation |
| **WLTP** | Worldwide Harmonised Light Vehicles Test Procedure |

# Table of contents

# 1 Introduction

EVs are becoming increasingly prevalent worldwide, while conventional vehicles are losing their popularity. This shift is primarily driven by the significant energy efficiency of electric motors and the lower life-cycle emissions compared to conventional fossil fuel vehicles [1]. As EV technology increasingly develops, the demand for precise simulation and testing environments has become critical for drivetrain development.

In this thesis, a high-performance EV driving system was designed and simulated by utilizing Typhoon HIL -software. This allows for real-time simulation, bridging the gap between theoretical modelling and physical implementation. The focus of the research was on the PMSM, specifically the interior PMSM design used in EVs like Hyundai Ioniq 5. This thesis explores the implementation of FOC and analyses the technical challenges related to signal synchronization and numerical integration in a real-time simulation environment.

In this thesis, the author has utilized Google Gemini to check and improve the English language. After using this tool, the author has checked and fixed the text and takes full responsibility for the thesis content.

# 2 Theoretical Background

## 2.1 Architecture and Components of an Electric Vehicle

EV's powertrain consists of three main components: the battery, electric motor and power transmission.

### 2.1.1 Battery and Battery Management System

The battery is the heart of the EV, functioning as its primary energy storage system and enabling propulsion by converting chemical energy into electrical energy. The battery pack is typically located under the vehicle floor in a durable case. Currently, batteries are mainly made of lithium-ion, as they have many advantageous features, including high energy density and low self-discharge time [2].

A battery pack consists of individual cells and modules. A single lithium-ion cell provides a nominal voltage of approximately 3,7 V and nominal current 3400 mAh. Cells are connected in series to increase voltage and to increase current, in parallel. Multiple cells form a module and several modules connected in series form the full battery pack [2]. Contemporary EV batteries operate with nominal voltages ranging from 400 V up to 800 V and higher voltage levels enable greater power output due to the linear dependence:

$$P = VI \tag{1}$$

The full capacity of the battery is not entirely fully usable. The total amount of energy the battery contains is referred to as the total capacity, whereas the portion available for actual use is the net capacity [3]. The difference between these values forms a buffer, which ensures that charging and discharging never reach neither 0 % nor 100 %. Maintaining this buffer is essential for preventing harmful overcharge and over-discharge events, thereby enhancing battery lifetime and performance [2].

The battery management system plays an essential role in controlling the buffer and ensuring safe operation. By choosing appropriate algorithms and circuit configurations, the BMS manages battery safety, reliability and durability [4]. Typical BMS functions include continuous monitoring of cell voltages, battery pack current and temperature distribution, as well as controlling charge/discharge limits and detecting fault conditions, such as fires or thermal runaways [2,5].

### 2.1.2 Electric Motor

Electric motor is the main component needed to convert electrical energy into mechanical energy in an EV. Most used motor types in EVs are PMSM, IM and BLCD motors. However, use of DC motors has become rare in modern EV applications due to their lower power density, relatively high maintenance and mechanical commutations. These disadvantages limit their performance and reliability compared to AC motor technologies [6]. PMSM motors will be discussed in more detail in Chapter 2.2.

Electric motor is a superior choice to use in EV propulsion for several reasons. Their energy efficiency commonly ranges between 80-96 % and they can deliver nearly constant torque over a wide speed range, which eliminates the need of a multi-speed transmission. They are also environmentally friendly and provide smooth and quiet operation [6].

Regardless of the motor type, all electric motors share the same two fundamental components:

- rotor, the rotating part
- stator, the stationary part

The working principle of electric motors is similar regardless of the motor type and is based on EMF. When an electric current flows through the stator windings, a MF is generated. This MF interacts with the MF of the rotor – either produced by induced currents or permanent magnets – causing the rotor to rotate. This rotation occurs because identical magnetic poles repel each other, creating continuous torque as the MF moves [6].

The mechanical energy produced by the electric motor is transferred through the drivetrain to the EV's wheels. To deliver smooth, powerful and environmentally friendly transportation, achieving optimal and torque and speed control across different driving conditions is crucial. Modern EV drivetrain designs typically use a single-speed reduction gear, enabled by the wide operating range and high torque availability of electric motors [6].

### 2.1.3 Power Transmission

EV's power transmission is responsible for transferring mechanical energy from the motor to the traction wheels. Usually, they employ a simplified transmission architecture because electric motors can operate efficiently across a very wide range of speed and deliver high torque from standstill. Electric motors, such as PMSM can produce maximum torque at 0

RPM. This removes the need for the multi-speed gearboxes typically required in ICE vehicles to maintain the engine within a narrow optimal operating band [7].

EVs typically use a single-speed step down transmission, whose primary purpose is to reduce the motor's high rotational speed to a wheel-appropriate speed while multiplying torque. This simplified drivetrain increases efficiency, reduces mechanical losses and minimizes maintenance due to the absence of clutches, synchronizers and gear-shifting components that are necessary in ICE-based transmissions [7].

Although PMSM differs from IM in construction and control, their torque-speed characteristics are similar in the context of vehicle drivetrains: high low-speed torque, wide constant-power region and efficient operation across a large speed band. Therefore, the engineering rationale presented in the review for using single-speed transmissions applies equivalently to PMSM-based EVs. Multi-speed transmission can offer marginal efficiency gains in some driving cycles, but as the review highlights, additional weight, cost and system complexity typically outweigh the benefits of practical EV design [7].

### 2.1.4 High-voltage System

High-voltage system forms an electric power line of an EV. Its primary purpose is to control, convert and transfer electrical energy between high-voltage battery, power electronics and the electric motor with minimal losses. The system typically includes battery, high-voltage relays, an inverter, a DC/DC converter and other high-voltage components [8]. As mentioned earlier, most current EVs operate at around 400 V, while the most advanced and efficient models use 800 V. A higher voltage level enables thinner and lighter cables and allows more efficient battery design [9].

A key component of the system is the inverter (inverted rectifier). Because the battery supplies DC power while a PMSM requires three-phase AC, the inverter controls the motor's rotational speed by adjusting the frequency and amplitude of the AC output. The inverter also operates in the opposite direction during regenerative breaking, converting the AC generated by the motor back into suitable DC to recharge the battery.

Another critical component is the DC/DC converter. Although the EV's high-voltage system operates at several hundred volts, traditional auxiliary systems such as lighting, windshield wipers and infotainment require lower voltage of 12 V or 48 V [10,11]. The DC/DC converter

replaces the alternator familiar from ICE vehicles by safely stepping down the high voltage to supply safely the low-voltage network.

Safety is a main priority in high-voltage system. All high-voltage components and cables are marked with orange colour according to international standards to warn the maintenance personnel and rescue authorities of potential life-threatening voltages. The system is galvanically isolated from the EV's chassis continuously monitored through isolation resistance measurement. In the event of car accident, the safety electronics activate pyrotechnic disconnect devices, which instantly cut the current flow from the battery, making the EV voltage-less [8,12].

## 2.2 Permanent Magnet Synchronous Motor

PMSM is a synchronous AC motor in which the rotor magnetic field is produced by permanent magnets rather than electromagnetically excited windings. PMSMs eliminate rotor copper losses, because the rotor does not require current to establish magnetization. This significantly increases overall efficiency and reduces heat generation during operation. The absence of rotor current eliminates resistive losses, leading to significantly higher efficiency and reduced heat generation during operation [13,14].

Permanent magnets used in PMSMs – typically Neodymium-Iron-Boron or Samarium-Cobalt – provide a strong and stable magnetic field that enables high torque density and compact motor dimensions. These characteristics contribute to PMSM's superior performance compared with many other motor types, particularly in applications, such as EVs, where high efficiency and dynamic responsiveness are required [14].

### 2.2.1 Construction

The construction of PMSM is based on a rotor-stator assembly similar to that of a traditional induction motor. The key difference between these two motors is that the rotor incorporates high-energy permanent magnets instead of windings. The stator consists of three-phase windings that generate a rotating magnetic field, while the rotor carries the permanent magnets made from high-performance magnet materials. These magnet materials provide strong magnetic excitation and maintain stability across varying temperatures and operating conditions [15].

PMSM rotor designs are generally classified into two main categories, depending on the magnet placement. Structural differences are visualised in figure 1.

**Surface-Mounted PMSM (SPMSM):**

In SPMSMs, the magnets are fixed directly onto the outer surface of the rotor iron core, typically in a circular array. This arrangement allows a magnetic field that interacts directly with the stator field to produce electromagnetic torque. This design is simply both in construction and magnetic behaviour, since the magnetic field distribution is nearly sinusoidal. The air gap between rotor and stator is uniform, resulting in smooth torque production and low cogging torque [16,17].

**Interior PMSM (IPMSM):**

An IPMSM differs significantly in rotor design compared to SPMSM. The permanent magnets are embedded within the rotor's iron core, often arranged in V- or U-shaped configurations. Magnetic saliency is introduced by this structural choice – a difference between the rotor's direct-axis (d-axis) and quadrature-axis (q-axis) inductances. Due to the magnetic saliency, IPMSMs generate not only magnetic torque but also reluctance torque, resulting in higher overall torque density. Furthermore, embedded magnets resist mechanical stress and demagnetization, making the design particularly robust for high-speed applications [16,17].

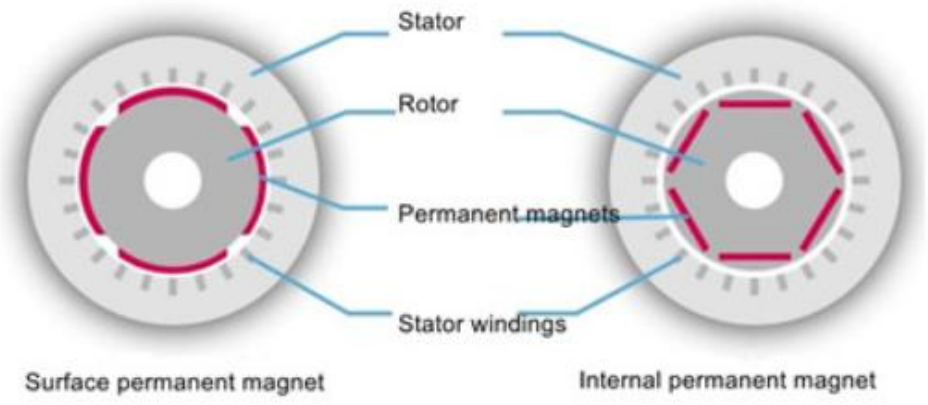


*Figure 1 Structural differences between surface (left) and interior permanent magnets [16]*

### 2.2.2 Working Principle

The operation of PMSM in EVs is fundamentally based on the magnetic interaction between the stator's rotating magnetic field and the rotor's permanent magnets. PMSMs are widely used in EV traction applications duef to their high efficiency, high torque density and precise controllability, which stem from the absence of rotor copper losses and ability to maintain synchronous rotation under all load conditions.

In EV applications, the motor is supplied by a power electronics inverter rather than relying on a squirrel-cage winding for asynchronous starting. This inverter generates controlled three-phase AC currents, establishing a rotating magnetic field whose frequency and phase are synchronized with the rotor position. The information of the rotor position is provided by sensors or observer algorithms, enabling fully synchronous operation from standstill to maximum speed without the need for induction-based startup torque.

When the motor is started, the stator's three-phase symmetrical current produces a rotating magnetic field. The rotor remains locked in synchronism from the very first rotation, because the inverter continuously adjusts this field based on rotor position feedback. This eliminates slip and ensures stable torque production throughout the operating range. PMSMs therefore offer smooth torque characteristics and minimal torque ripple, which are essential for EV drivability, energy efficiency and noise, vibration and harshness performance.

Torque generation arises from the controlled angular displacement – the torque angle – between the stator magnetic field and the rotor permanent magnet field. For achieving high efficiency, dynamic responsiveness and operational stability, maintaining the torque angle within an optimal range is crucial. Modern PMSM field-oriented control and direct torque control strategies are designed specifically to regulate this magnetic alignment under varying load and speed conditions.

When the rotor no longer induces current because its magnetic field is entirely produced by permanent magnets, the steady-state synchronous operation is achieved. The torque is generated solely through the interaction of the rotor's magnet field and the stator's rotating field. This characteristic contributes to PMSM's high power density, wide constant-power speed range and superior efficiency compared to induction and switched reluctance machines, making it the leading motor type for modern EV powertrains [18].

### 2.2.3 Advantages and Disadvantages

PMSM has many advantages. Perhaps the most significant one is the high efficiency, which varies from 92 % to 97 % [19]. This is because the structure of the motor. The rotor is equipped with permanent magnets, which does not require additional current to generate magnetic field, thus reducing energy loss.

Comparing to other motors, PMSM has the highest power density, meaning that it can output more power under the same volume and weight. When motors of equal size and rating are compared, PMSMs deliver 29,9 % higher density than BLDC motors, 88,7 % higher than SRM machines and 200 % higher than induction motors. This results from the strong and constant air-gap flux provided by permanent magnets, combined with the low rotor inertia, which also gives PMSMs excellent dynamic response and smooth torque production over a wide speed range [20].

The reliability of PMSM is also very high, which is a result of the simple structure of the motor. Because it has no winding, there is no problem of winding short circuit or broken wire. Secondly, no affections by environmental factors such as temperature and humidity will occur, because the magnetic properties of permanent magnets are very stable. Finally, the control system of PMSM is relatively simple and the failure rate is low. Other advantages are low noise, good speed regulation performance and high adaptability.

Despite these advantages PMSM provides, it has some disadvantages as well. PMSMs are highly sensitive to parameter variations, such as resistance, inductance and magnetic flux. These parameters change significantly with temperature, saturation and operating conditions, which complicate accurate control and may degrade overall performance of the motor. Temperature also affects on magnet performance. As it increases, the magnet strength reduces and changes the machine parameters, potentially lowering the efficiency [21].

The control requirements of PMSMs are also complex and advanced, including MTPA, MTPV, field-weakening and sensorless algorithms. To achieve optimal performance, these control strategies are needed. PMSM relies also heavily on precise rotor position estimation [21]. Sensorless control methods become inaccurate at low speed or under difficult operating conditions, which can cause torque ripple, instability, or loss of synchronism.

PMSM drives are more vulnerable to external disturbances, parameter mismatches and load fluctuations. These issues can lead to current tracking errors, increased torque ripple and

degraded dynamic behaviour unless control challenges and potentially lowering efficiency. Lastly, PMSMs are relatively expensive, as they require high-performance power electronics. Installation of the permanent magnets to the rotor is a high cost as well.

## 2.3 Driving Cycles

Driving cycle is a standardised speed-time profile used to represent typical vehicle operation in real-world conditions. Understanding driving cycles is essential when developing and designing EVs, as they define how key components introduced in earlier chapters – such as battery, power electronics and PMSM – perform under dynamic driving demands. Unlike ICE vehicles, the efficiency and energy consumption of EVs vary significantly depending on whether the cycle emphasises low-speed urban driving or continuous high-speed operation.

### 2.3.1 Standards and Testing Methods

International testing standards have been established to enable comparable evaluations of EV range and energy consumption across manufacturers. In Europe, the most relevant procedure is the WLTP-standard, which replaced the earlier NECD-cycle due to the latter's unrealistically optimistic results. Since 2018, all new EV models sold in Europe must be tested according to WLTP. Compared to NECD, the WLTP cycle includes more dynamic driving behaviour and better represents various real—world conditions [22]. The United States uses the EPA-cycle, while China applies the CLTC-cycle. Four phases of WLTP-cycle are described in table 1 and differences between WLTP and NEDC in table 2.

*Table 1 Four phases of WLTP*

| **Phase** | **Description** |
|---|---|
| Low (Urban) | Characterised by low speeds and frequent stops and accelerations decelerations. Regenerative braking is most effective in this phase, significantly reducing energy consumption. |
| Medium (Sub-Urban) | Driving becomes steadier with fewer stops and a higher average speed. Aerodynamic drag begins to have a greater influence compared to the Urban phase. |

| | |
|---|---|
| High (Main Road) | Speeds approach 100 km/h, resulting in higher power demand. The PMSM operates at increased torque and speed and efficiency depends strongly on the motor's operating point. |
| Extra High (Highway) | Speeds up to 131 km/h. Aerodynamic drag becomes the dominant load component and EV efficiency typically decreases most. Battery discharge power is highest in this phase. |

*Table 2 Differences between NEDC and WLTP cycles*

| **Feature** | **NEDC** | **WLTP** |
|---|---|---|
| Cycle Time | 20 min | 30 min |
| Cycle Distance | 11 km | 23,25 km |
| Avg. speed | 34 km/h | 46,5 km/h |
| Max. speed | 120 km/h | 131 km/h |
| Driving Phases | 2 (Urban, Extra-Urban) | 4 (Low, Medium, High, Extra High) |
| Stoppages of time | 25 % | 13 % |

The increased dynamism of WLTP-cycle is evident from its higher average speed and reduced idle time. From an EV perspective, this results on a more continuous and evenly distributed load on the battery. The PMSM must also be able to operate over a wider speed and torque range for longer periods. Unlike NEDC, the WLTP procedure additionally accounts for optional equipment – such as larger wheels or sunroof – which affect vehicle mass and aerodynamics, thereby directly influencing energy consumption.

Although WLTP represents a clear improvement, it is important to note its limitations. The test is conducted at a standardised ambient temperature of 23 Celsius under laboratory conditions. Tests have shown that the real-time EV ranges are often 10-20 % lower than WLTP ratings due to two main factors [23]:

**Temperature variation**: At low temperatures, battery internal resistance increases, reducing efficiency. Additionally, cabin heating places a significant extra load on the high-voltage system.

**Aerodynamic drag:** At high speeds (Extra High phase), aerodynamic drag becomes a dominant energy consumption factor. This effect is more pronounced in EVs that lack multi-speed transmissions to optimise motor RPM.

# 3 Real-Time Simulation and HIL-technology

Real-time simulation is a key part of developing EV control systems because it enables the safe design, testing, verifying and validation of complex drivetrain, battery and charging functions without requiring a physical prototype. In a modern EV, systems such as the power inverter, BMS and DC/DC converters require precise and fast interaction with their environment. Real-time simulation provides the necessary computational fidelity to model these interactions accurately [24].

In HIL-technology, critical physical components of an EV are tested against real-time simulation. This makes it possible to reproduce driving situations, motor loads, behaviour and fault conditions in a safe and controlled environment. In EV development projects, HIL-testing provides several important advantages. It allows for the rigorous testing of inverter control algorithms without a physical motor and enables the simulation of cell-level battery behaviour for BMS validation. Furthermore, HIL-technology facilitates the testing of both AC and DC charging processes and provides a risk-free environment for simulating dangerous fault conditions, such as short circuits, cell imbalance or overheating.

## 3.1 Experimental Equipment

The experimental setup was based on the Typhoon HIL system, which provides an integrated platform for real-time power electronics simulation. The equipment consists of both software and hardware components:

**Typhoon HIL 101 Device:** A high-fidelity real-time emulator capable of simulating power electronics with ultra-low latency. The device utilizes FPGA-based solvers to execute the electrical model of the inverter and motor at very small-time steps. Figure 2 illustrates the device.

**Typhoon HIL Control Center:** The primary software used for designing and executing the simulation

- **Schematic Editor:** Used to build the electrical and control diagrams of the Ioniq 5 powertrain.
- **HIL SCADA:** Used to create a customized dashboard for real-time monitoring and control of variables such as motor speed, torque and phase currents.

**Host PC:** A standard workstation used to compile the schematic model into executable code for the HIL hardware and to log simulation data.

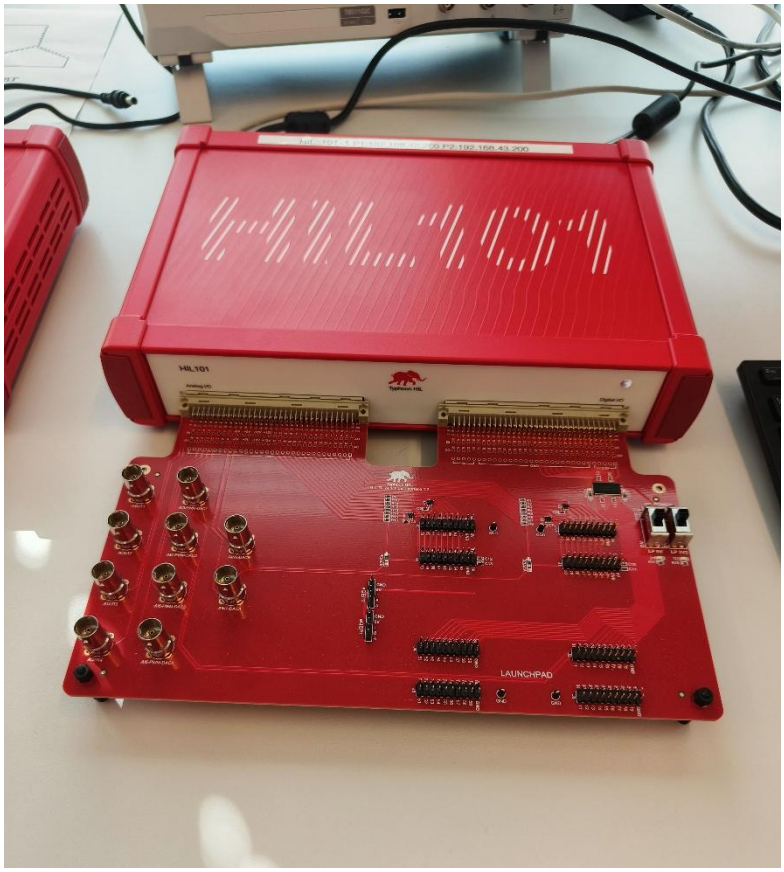


*Figure 2 Typhoon HIL 101 Device*

## 3.2 Procedure

The research followed a structured simulation workflow, moving from mathematical modelling to real-time hardware execution. The procedure was divided into the following steps:

1. **Modelling and Parameterization:** The physical components, including the 750 V battery, three-phase inverter, and the IPMSM motor, were defined in the Schematic Editor. Technical specifications from the Hyundai Ioniq 5 [25] were utilized to set the motor's inductance $L_d, L_q$, resistance $R_s$ and permanent magnet flux linkage.

2. **Control Logic Implementation:** The FOC algorithm and PI-controllers for speed and current were utilized from a ready PMSM example model and modified to correspond to EV purposes.

3. **Compilation and Loading:** The completed schematic was compiled into real-time executable. During this stage, the software mapped the electrical components to the HIL device's FGPA solvers and the control logic to the CPU.

4. **Real-Time Execution and Testing:** The model was executed on the HIL hardware. The HIL SCADA Dashboard was used to provide reference commands (e.g. target speed and current) and to monitor the system's response.

5. **Data Acquisition and Analysis**: Performance data, including phase currents and the electrical angle $\theta$ were captured using the built-in data logger. These results were then exported for further analysis and identification the synchronization and modulation challenges discussed in chapter 5.

# 4 Implementation and Validation of the Simulation

In this chapter, the technical implementation of the simulation model in Typhoon HIL - environment is described. Additionally, the methods that ensured numerical stability and physical accuracy of the model are explained. The simulated model focuses on the powertrain of a Hyundai Ioniq 5 EV shown in figure 3, controlled according to the WLTP driving cycle.

*Figure 3 Hyundai Ioniq 5*

## 4.1 Simulation Environment and Model Structure

The simulation model was built using Typhoon HIL Control Center software in schematic editor mode. The model consists of three main components: the electrical power stage, the control system and the mechanical load model.

The electrical power stage includes a DC voltage source, a three-phase inverter and PMSM. The motor parameters were set to match the technical specifications of the Ioniq 5, accounting for the number of pole pairs, stator inductances and torque constant.

## 4.2 Control Strategy and Parameterisation

FOC was utilized for motor control. The control structure consists of two main parts:

1. Speed Control: compares the reference speed $w_{ref}$ from the WLTP profile to the actual motor speed and calculates the required reference current $i_{q,ref}$

2. Current Control: Regulates the d- and q-axis currents ($i_d, i_q$) by adjusting the inverter switching states using SVPWM.

To balance response time and stability, PI-controllers were used with optimised parameters. Special attention was paid to the anti-windup logic of the integrators and the limitation of the current reference to ensure the system remains stable during aggressive acceleration.

## 4.3 Refinements for Numerical Stability

Significant numerical instabilities were observed during the development phase, which lead to simulation crashes (Arithmetic Overflow or NaN errors). To resolve these issues and validate the model, the following critical technical adjustments were made:

- Standardisation of the DC Source: An ideal 750 V DC source was used to replace the original dynamic battery model. This eliminated voltage fluctuations caused by internal resistance and discharge curves, which previously triggered numerical singularities in the inverter control logic.

- Mechanical Model Calculation Algorithms: The power block $u^v$ used for calculating air resistance was replaced with a more stable production block $v * v$. This prevented mathematical error states in scenarios where speed value momentarily fluctuated below zero during braking.

- Integrator Saturation: Saturation limits (0 … 100 m/s) were added to the speed integrator. These limits prevented unrealistic speed values and numerical divergence during the long standstill periods in the WLTP cycle.

## 4.4 Validation using the WLTP Cycle

Before starting the simulation, the WLTP speed profile was imported into the Typhoon environment as a time-series dataset. This dataset was linked to a lookup table, which provided the instantaneous reference velocity $v_{ref}$ to the speed control loop. This velocity vas converted from km/h to rad/s to serve as the angular velocity reference $w_{ref}$ for the motor controller.

The simulation run focused on the first 1800 seconds of the cycle. The vehicle model utilized the rolling resistance, aerodynamic drag and mass parameters of the Hyundai Ioniq 5. The objective was to observe the current controller's ability to track the rapidly chancing torque demands required to follow the WLTP profile.

# 5 Results and Evaluation

The developed motor control mode is evaluated based on initial simulation runs in this section. Parameters from the Hyundai Ioniq 5 EV motor were utilized for the simulation setup. The motor was powered by a 750 V battery. The primary objective was to examine the performance of the EV in different driving phases of WLTP-cycle. The overall model is shown in figure 4.

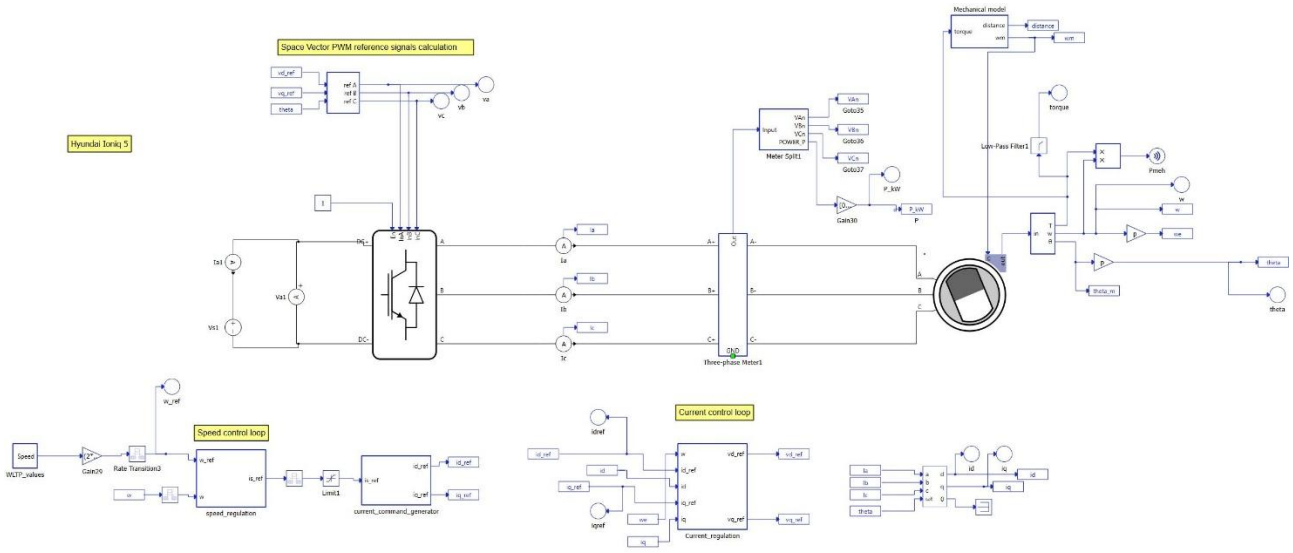


*Figure 4 The overall model*

## 5.1 Control Instability and Current Discrepancy

Initial results indicated a significant discrepancy between the control commands and the actual motor behaviour. This was observed across both virtual simulation and HIL-testing phases. Although the phase currents $I_a, I_b$ and $I_c$ were non-zero, they failed to track the reference commands $I_{q,ref}$ generated by the speed controller.

In an ideal FOC system, the current vector must be maintained at a 90° angle relative to the rotor magnetic flux to maximize torque production. In this simulation, the feedback loop provided an incorrect electrical angle, which caused the current vector to become misaligned or stagnant.

## 5.2 Field Orientation and Torque Stability

The electromagnetic torque produced by the motor stabilised at approximately 3,44 Nm. However, the torque fluctuated between positive and negative values, exhibiting notable instability.

The root cause for the instability was identified as a synchronisation failure in the electrical angle $\theta$ feedback loop. During the simulation, theta remained stagnant at 0 or 6,28 rad, indicating that the integration of mechanical speed into electrical position was not successfully relayed to the Park and Inverse Park transforms. The FOC algorithm cannot maintain the correct orientation of the stator flux vector relative to the rotor magnets, without a dynamically updating theta. This led to inefficient torque production and torque ripple.

## 5.3 Mechanical Response and Power Output

The mechanical subsystem-model demonstrated logical behaviour despite the limitations in the electrical drive. Although the measured vehicle speed remained at 0 m/s, a transient peak mechanical power of approximately 1,3 kW was observed during the initial moment of the simulation. This peak validates the integration of the vehicle dynamics equations and the processing of torque within the model, even though the electrical drive was unable to sustain movement due to the $\theta$-angle integration failure. The results highlight the significant differences between in time constants between the fast electrical control and the slower mechanical response of the vehicle.

## 5.4 Behaviour and Limitations of the WLTP-cycle

During the simulation runs it was revealed that while the control architecture successfully received the speed references from the WLTP cycle, the electrical drivetrain struggled with the high-dynamic transitions of the cycle. As analysed in previous subsections, the synchronisation issues in the $\theta$-loop caused the motor to produce inefficient torque to keep up with aggressive acceleration phases of the WLTP-cycle. This resulted the vehicle speed to remain at 0 m/s.

However, the integration of the WLTP block into the Typhoon HIL environment was successfully validated. As intended, the signal chain from the driving cycle data to the current command generator functioned appropriately. This demonstrated that the model structure is capable of full-cycle simulation once the angular synchronisation is further refined.

# 6 Conclusion

The primary objective of this thesis was to develop a real-time simulation model for the Hyundai Ioniq 5 EV powertrain using the Typhoon HIL environment. The work focused on implementing FOC algorithm to drive an IPMSM and integrating it with a vehicle dynamics model.

The simulation demonstrated that while the mechanical subsystem and vehicle parameters and equations were correctly configured to respond to torque inputs, the electrical control loop faced significant synchronization challenges. The most critical observation was the sensitivity of the FOC algorithm to the accuracy and continuity of the electrical angle $\theta$ feedback. The stagnant or low torque and low phase currents observed during simulations were traced back to two primary factors: the lack of modulo-arithmetic in the angular integration and the requirement for explicit PWM modulation in a high-fidelity real-time inverter model.

Despite the limitations in vehicle acceleration during testing-phase, the simulation successfully established a functional framework. The study highlights the fundamental differences between virtual simulations and the precise timing and signal-dimension requirements of real-time HIL-testing. These observations proof the demanding nature of EV modelling and testing in real industry.

For further development it is recommended to update the control logic with an integrator that resets after each rotation ($0 \ldots 2\pi$). Additionally, the motor position sensing should be made more precise to improve the overall control accuracy. Furthermore, fine-tuning the PWM carrier frequency and the sampling rates of the current controllers would likely resolve the remaining discrepancies between the reference commands and the actual motor behaviour. In conclusion, the simulation work serves as an extensive exploration into the complexities of modern EV drivetrain emulation and provides a structured methodology for debugging high-performance motor controllers.

.

## References


[1] Global EV Outlook 2025, (2025).

[2] M.S. Ramkumar, C.S.R. Reddy, A. Ramakrishnan, K. Raja, S. Pushpa, S. Jose, M. Jayakumar, Review on Li-Ion Battery with Battery Management System in Electrical Vehicle, Adv. Mater. Sci. Eng. 2022 (2022) 1–8. https://doi.org/10.1155/2022/3379574.

[3] H. Bašić, V. Bobanac, H. Pandžić, Determination of Lithium-Ion Battery Capacity for Practical Applications, Batteries 9 (2023) 459. https://doi.org/10.3390/batteries9090459.

[4] L. Schärtel, B. Reick, M. Pfeil, R. Stetter, Analysis and Synthesis of Architectures for Automotive Battery Management Systems, Appl. Sci. 12 (2022) 10756. https://doi.org/10.3390/app122110756.

[5] A. Kurkin, A. Chivenkov, D. Aleshin, I. Trofimov, A. Shalukho, D. Vilkov, Battery Management System for Electric Vehicles: Comprehensive Review of Circuitry Configuration and Algorithms, World Electr. Veh. J. 16 (2025) 451. https://doi.org/10.3390/wevj16080451.

[6] H. El Hadraoui, M. Zegrari, A. Chebak, O. Laayati, N. Guennouni, A Multi-Criteria Analysis and Trends of Electric Motors for Electric Vehicles, World Electr. Veh. J. 13 (2022) 65. https://doi.org/10.3390/wevj13040065.

[7] M.I. Jamadar, S.S. Shainde, F.J. Badshah, S.S. Sawant, R.J. Gundla, Review on Electric Vehicle Transmission System, 7 (2020).

[8] High voltage - Basic information, (n.d.). https://www.ms-motorservice.com/int/en/technipedia/high-voltage-basic-information (accessed February 22, 2026).

[9] H. Qing, High Voltage Electric Vehicles, MSc Thesis, University of Vaasa, 2024.

[10] A. Bagheri, A. Parastar, DCDC Power Conversion System in Electric Vehicle Part 2: Design and Development, (2025).

[11] Safe Handling of High Voltage Electrical components in Electrical End of Life Vehicles, (n.d.). https://www.globalsuzuki.com/xev_battery/download/pdf/idis_common_hv_en.pdf (accessed February 22, 2026).

[12] P. Kurian, M. Abbasian, Investigating High-Voltage Safety Concerns in Electric Vehicles Through Voltage Discharge Optimisation, Energies 18 (2025) 916. https://doi.org/10.3390/en18040916.

[13] E. Kinoti, T.C. Mosetlhe, A.A. Yusuff, Multi-Criteria Analysis of Electric Vehicle Motor Technologies: A Review, World Electr. Veh. J. 15 (2024) 541. https://doi.org/10.3390/wevj15120541.

[14] W. Sun, H. Si, J. Qiu, J. Li, Research on Efficiency of Permanent-Magnet Synchronous Motor Based on Adaptive Algorithm of Fuzzy Control, Sustainability 16 (2024) 1253. https://doi.org/10.3390/su16031253.

[15] N. Shaik, Design and Comparison of Permanent Magnet Motor Topologies for Different Application Sectors, MSc Thesis, 2022.

[16] Surface-Mounted vs Interior Permanent Magnet Synchronous Motors: Key Differences – Leili Motor, (n.d.). https://www.leili-motor.net/surface-mounted-vs-interior-permanent-magnet-synchronous-motors-key-differences/ (accessed February 19, 2026).

[17] W.-S. Jung, H.-K. Lee, Y.-K. Lee, S.-M. Kim, J.-I. Lee, J.-Y. Choi, Analysis and Comparison of Permanent Magnet Synchronous Motors According to Rotor Type under the Same Design Specifications, Energies 16 (2023) 1306. https://doi.org/10.3390/en16031306.

[18] V. Zamani faradonbeh, M. Alaei Faradonbeh, A. Rashidi, Design of Permanent Magnet Synchronous Motor PMSM) for use in electric vehicle EV), Electromechanical Energy Convers. Syst. (2025). https://doi.org/10.30503/eecs.2024.483451.1063.

[19] K. Dambrauskas, J. Vanagas, T. Zimnickas, A. Kalvaitis, M. Ažubalis, A Method for Efficiency Determination of Permanent Magnet Synchronous Motor, Energies 13 (2020) 1004. https://doi.org/10.3390/en13041004.

[20] Simon Fekadeamlak Gebremariam, Tebeje Tesfaw Wondie, Comparative analysis of electric motor drives employed for propulsion purpose of Battery Electric Vehicle (BEV) systems, Int. J. Sci. Res. Arch. 10 (2023) 1097–1112. https://doi.org/10.30574/ijsra.2023.10.2.1074.

[21] HIL Testing Electric Vehicle Drive Units, Typhoon HIL (2022). https://www.typhoon-hil.com/blog/hil-testing-ev-drive-pmsm/ (accessed April 10, 2026).

[22] WLTP Explained, EVDB (n.d.). https://evdb.nz/wltp (accessed February 23, 2026).

[23] Garratt, Ellie, Electric Car Range Explained 2026 | WLTP vs Real-World, Electr. Car Scheme (2025). https://www.electriccarscheme.com/blog/electric-car-range (accessed April 12, 2026).

[24] M. Abboush, D. Bamal, C. Knieke, A. Rausch, Hardware-in-the-Loop-Based Real-Time Fault Injection Framework for Dynamic Behavior Analysis of Automotive Software Systems, Sensors 22 (2022) 1360. https://doi.org/10.3390/s22041360.

[25] Hyundai Motor Company, 2026-IONIQ-5-Specification-Sheet, (2026).

# Appendices

## Appendix 1 Vehicle and Motor Parameters in Typhoon

```
# Numpy module is imported as 'np'
# Scipy module is imported as 'sp'
# The Schematic API is imported as 'mdl'
# To get the model file path, use 'mdl.get_model_file_path()'
# To print information to the console, use info()

import numpy as np
import math

# --- 1. GENERAL SETTINGS ---
Ts = 100e-6          # [s] Control loop execution rate (10 kHz)
fsw = 10000.0        # [Hz] Inverter switching frequency
dt = 1e-6            # [s] Inverter dead time

# --- 2. VEHICLE DYNAMICS (Hyundai Ioniq 5) ---
# For calculating drag and accelerationg inside Mechanical model -subsystem
max_speed = 185          # [km/h] vehicle max speed
vehicle_mass = 2065.0      # [kg] vehicle tare mass
wheel_diameter = 0.741    # [m] wheel diameter
gear_ratio = 10.65        # gear ratio (2.263 * 4.706, front * rear)
transmission_eff = 0.97  # transmission efficiency
front_area = 2.58         # [m^2] front_area (for drag)
drag_coeff = 0.288        # drag coefficient
rolling_coeff = 0.012    # rolling coefficient
braking_force = 20e3     # [N] max breaking force

# --- 3. MOTOR PARAMETERS (Hyundai Ioniq 5) ---
Pn = 168000.0    # [W] max power
Vn = 697.0       # [V] rated voltage (DC)
In = 400.0       # [A] rated current (DC)
Rs = 0.012        # [Ohm] stator resistance
Ld = 1.6e-4      # [H] d-inductance
Lq = 4.2e-4      # [H] q-inductance
J = 2.0         # [kg*m^2] moment of inertia
n_n = 4500.0     # [rpm] rated speed
p = 4            # pole pairs
f = n_n*p/60     # [Hz] rated electrical frequency
psi_pm = 0.2    # [Wb] pm flux linkage
Back_emf = psi_pm*np.pi*1000/30*p    # [V] back EMF at 1000 rpm
n_back_emf = 1000    # [rpm]

# --- 4. PI-CONTROLLER  (Current Controller) ---
# These automatically calculate correct Kp and Ki values for the
# current control loop regarding to L and R
fcc = fsw / 25.0
wcc = 2.0 * np.pi * fcc

Kpid = Ld * wcc  # d-axis Proportional
Kiid = Rs * wcc  # d-axis Integral
Kpiq = Lq * wcc  # q-axis Proportional
Kiiq = Rs * wcc  # q-axis Integral
```